Acta Cryst. (1960). **13**, 919

The Structure of Muscovite, $KAl_2(Si_3Al)O_{10}(OH)_2$

By E. W. Radoslovich

Division of Soils, Commonwealth Scientific and Industrial Research Organization, Adelaide, Australia

(*Received* 27 *October* 1959)

The structure of the $2M_1$ polymorph of muscovite, originally described by Jackson & West (1930, 1933), has been refined. The new atomic parameters show the structure to be considerably distorted from the ideal structure, especially by a departure from hexagonal symmetry on the surfaces of the silicate sheets. A number of difficulties concerning muscovite can now be resolved, and tentative explanations offered for properties of other layer silicates.

Though the structures of the micaceous minerals have been known in their main features for many years there is now considerable interest in the precise details of these and related layer-lattice silicate structures, especially the clay minerals.

The unit cells and symmetries of the micas were first investigated by Mauguin (1928). Their general structural scheme was then proposed by Pauling (1930) from a consideration of these dimensions, and of the known layer structures of the related minerals hydrargillite (i.e. gibbsite) $Al(OH)_3$, brucite $Mg(OH)_2$, β-tridymite SiO_2 and β-cristobalite SiO_2. Pauling showed that the micas also are layer structures, with an octahedral Al–O layer between two tetrahedral Si–O layers.* At the same time Jackson & West (1930, 1933) studied muscovite ($KAl_2(Si_3Al)O_{10}(OH)_2$) further, investigating the relative positions of the layers in the x and y directions. Their structure, based on symmetry and packing considerations, was confirmed by a general comparison of the observed and calculated intensities of a limited number of *hkl* reflections. This work was not claimed to give atomic parameters accurately, however, the structure being essentially an 'ideal' one.

No other analyses of mica structures appear to have been made since that of Jackson & West; and indeed it is only recently that structure analyses have been made of any layer-lattice silicates. Of these analyses the most accurate work is that on vermiculite by Mathieson & Walker (1954), and by Mathieson (1958). Less precise analyses have also been reported of amesite (Steinfink & Brunton, 1956), dickite (Newnham & Brindley, 1956), chloritoid (Harrison & Brindley, 1957), prochlorite (Steinfink, 1958*a*) and corundophillite (Steinfink, 1958*b*).

The ideal muscovite structure of Jackson & West (1930) leaves several problems unsolved, viz.:

(*a*) For the accepted space group ($C2/c$) and ideal structure, reflections of the kind $06l$, with l odd, are forbidden; but such reflections are observed.

(*b*) The measured monoclinic angles for many layer-lattice silicates (e.g. muscovite) do not agree with the ideal angles, $\beta = \cos^{-1}(-a/3c)$.

(*c*) There is a known misfit between the dimensions of a 'free' tetrahedral Si–O (or a $Si_{\frac{3}{4}}Al_{\frac{1}{4}}$–O) layer and a 'free' octahedral Al–O layer, and this misfit must somehow be accommodated in muscovite.

(*d*) Jackson & West gave the K–O bondlength as 3·09 Å, which is rather larger than the sum of their ionic radii, 2·95 Å approx. if the K^+ is 12-coordinated.

(*e*) In the tetrahedral layers the four cation sites are occupied by 3 Si and 1 Al ion; are these in an ordered arrangement?

(*f*) Hendricks & Jefferson (1939), and later Levinson (1953) and others, have demonstrated extensive polymorphism amongst the micas, whilst Smith & Yoder (1956) have recently suggested a theory to predict possible polymorphs. Some of these are either rare or not yet observed, but there appears to be no satisfactory explanation either of this or of the relative abundance of the common polymorphs.

Hendricks & Jefferson (1939) suggested that muscovite is unique among the micas in possessing only one form, the two-layer monoclinic form ($2M_1$) studied by Jackson & West (1930). This is no longer accepted, but since the $2M_1$ polymorph is the most common it is the one chosen for the present re-examination of the muscovite structure. Yoder & Eugster (1955) give cell dimensions for a synthetic $2M_1$ muscovite as

$$a = 5{\cdot}189 \pm 0{\cdot}010,\ b = 8{\cdot}995 \pm 0{\cdot}020,$$
$$c = 20{\cdot}097 \pm 0{\cdot}005\ \text{Å},\ \beta = 95^\circ\ 11' \pm 5'.$$

This contains four formula units, $KAl_2(Si_3Al)O_{10}(OH)_2$. The systematically absent reflections are consistent with either the space-group $C2/c$ or the non-centrosymmetric equivalent, Cc; and in absence of evidence for asymmetry Jackson & West chose $C2/c$. (Pabst (1955) has recently proposed that the one-layer micas are best described as $C2/m$, not Cm). The density is $2{\cdot}83_1$ g.cm.$^{-3}$, calculated from the unit-cell dimensions and molecular weight.

* The structural features of micas are adequately described by Bragg (1937).

Experimental

The sample of muscovite studied was from the Spotted Tiger Mine, Central Australia. The hand specimen consists of felspar crystals and of hexagonal muscovite books, 3 to 4 cm. across, which had grown into a cority. The muscovite is attached to the felspar, which is corroded in places. The books are clear at the edges, but show greenish iron stains in cleavage planes toward the centre. A suitable flake ($0{\cdot}4 \times 0{\cdot}5 \times 0{\cdot}1$ mm. approx.) was cut parallel to the true a-axis, from the edge of one book; the orientation was checked by the interfacial angles on the book, by percussion figures, and by Laue photographs. The true a-axis may be chosen optically and is confirmed by an oscillation photo after aligning the crystal about c, normal to the flake. (A 5° tilt towards $-a$ gives layer-lines for a 20 Å c-axis, but a tilt towards a pseudo a-axis gives layer-lines for a 60 Å spacing, given by the larger orthorhombic cell).

The refractive indices have the values

$$\beta = 1{\cdot}594 \pm 0{\cdot}001, \quad \gamma = 1{\cdot}598 \pm 0{\cdot}001$$

which suggests a fairly pure muscovite. A chemical analysis on a powdered sample, obtained by filing a mica book, gave the results in Table 1.

Table 1. *Chemical analysis of muscovite from Harts Range, Central Australia*

	%	No. of metal ions	No. of oxygens	Metal ions* (22 oxygens)	
K_2O	10·91	0·2316	0·1158	1·872	1·987
Na_2O	0·44	0·0142	0·0071	0·115	
SiO_2	46·20	0·7675	1·5350	6·220	8·000
Al_2O_3	34·28	0·6722	1·0083	5·450	+
Fe_2O_3	2·29	0·0288	0·0432	0·237	4·018
MgO	0·60	0·0149	0·0149	0·121	
H_2O	5·0			4	
	99·72				

Analyst: R. Bond, Division of Soils, C.S.I.R.O., Adelaide.

* Calculated on the basis of 22 oxygens in the unit cell, ignoring H_2O. The percentage of Fe_2O_3 is difficult to determine, since there is a marked variability across any mica book, due to the iron stains. An estimate of 2·6% Fe_2O_3 was formed from the value of the refractive indices. Fluorescent X-ray spectrography on the powdered sample gave 2·1%, though values from 1·5% to 2·5% were found on scanning a 'book' of mica with a fine beam.

It is quite difficult to prepare a small muscovite crystal which is free from distortion or attached fragments, and it is not possible (due to the marked cleavage) to grind such a crystal to an ideal shape. The crystal used is sufficiently small, however, for the absorption not to vary seriously for different reflections (using Mo $K\alpha$ radiation for which $\mu/\varrho = 4{\cdot}8$ approx.). A diffractometer pattern of the powdered specimen was compared with the curves of Yoder & Eugster (1955) to confirm that this muscovite is a $2M_1$ polymorph.

Weissenberg photographs were taken on a Nonius integrating goniometer about the a-axis (zero to 7th layer lines), b-axis (zero, 1st, 3rd, and 5th) and c-axis (zero layer). On these photographs about 900 independent reflections are permissible for space group $C2/c$, of which 550 were observed. About 200 of these were measured on both a- and b-axis photographs. The integrated intensities were measured using a microphotometer in which the slits were adjusted to be smaller than the flat plateau of density on the integrated reflections; the film density is then proportional to the integrated intensity. Two independent measurements of the $0kl$ intensities, some weeks apart, gave agreement to better than 10%; a pack of three films, interleaved with tin foil, was used for each photograph. The a-axis photographs were correlated using the b-axis photographs, though due to the systematic absences the $0kl$ reflections could only be correlated by taking a *combined* $0kl$ and $1kl$ photograph, with a wide slot in the layer-line screen. The Lorentz and polarization corrections were applied to the correlated intensities graphically. Since the weakest reflections were hard to measure after integration the a-axis photographs were repeated using long exposures, without integration, from which reflections could be assessed as 'weak-but-present' or as absent. The systematic absences were therefore confirmed; no hkl reflections of the kind $(h+k)$ odd are observed. A powdered sample of the Spotted Tiger muscovite, mixed with a standard quartz sample, was photographed on a carefully calibrated 19 cm. vacuum powder camera, for comparison with the unit-cell dimensions reported for synthetic muscovite. The b- and c-axes were determined as $8{\cdot}996 \pm 0{\cdot}006$ Å and $20{\cdot}096 \pm 0{\cdot}02$ Å respectively, assuming $\beta = 95°\ 11'$.

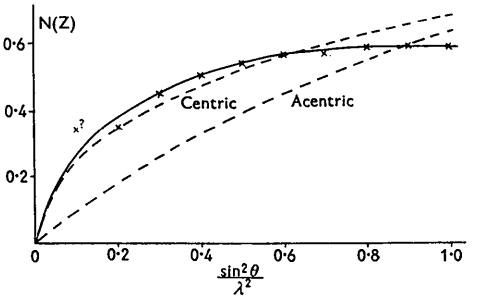

Fig. 1. Wilson's N(2) test for centrosymmetry, applied to one zone of general reflections for muscovite.

Two statistical tests for centrosymmetry due to Wilson were applied to some general hkl reflections. For two such zones containing many reflections the Wilson ratio, $(\overline{F})^2/\overline{F^2}$, was 0·507 and 0·455. Whilst this is not good agreement with the theoretical value for centrosymmetry (0·637), these figures are still further removed from the acentric value (0·785). It was hoped to avoid effects due to hypersymmetry in the $N(Z)$ test (Steinfink & Brunton, 1956) by applying it to one zone of general (rather than $0kl$) reflections

(Fig. 1). Though the departure from the theoretical curve at high values of $\sin^2\theta/\lambda^2$ may indicate some effect of hypersymmetry the results show that muscovite is probably centrosymmetric. The intensities were placed on an absolute scale by Wilson's method, the factor being adjusted in later calculations.

Calculations

Jackson & West (1930) proposed that the space group of muscovite is $C2/c$, though they pointed out that the symmetry must be lower than this if the tetrahedral cations are fully ordered. The possibilities then are either Cc or $P2/c$, of which Cc is acentric and $P2/c$ would allow *all hkl* reflections, contrary to observation. The maximum order possible in the tetrahedral ions for $C2/c$ (assumed correct) is $2\ Si_{\frac{1}{2}}Al_{\frac{1}{2}}$ with 2 Si.* There are eight general positions in this space group, related by the symmetry operations of face-centring, a glide of $c/2$ after reflection across the plane at $y=0$, and a centre of symmetry at the origin. A suggested system of nomenclature for each atom is illustrated (for Si_1) in Table 2.

Table 2. *System of nomenclature.*

System of nomenclature for atoms

Si_1	(000)	x	y	z	Si_1	(0g0)	$\bar{x}$	y	$\frac{1}{2}-z$
Si_1	(00c)	$\bar{x}$	$\bar{y}$	$\bar{z}$	Si_1	(0gc)	x	$\bar{y}$	$\frac{1}{2}+z$
Si_1	(f00)	$\frac{1}{2}+x$	$\frac{1}{2}+y$	z	Si_1	(fg0)	$\frac{1}{2}-x$	$\frac{1}{2}+y$	$\frac{1}{2}-z$
Si_1	(f0c)	$\frac{1}{2}-x$	$\frac{1}{2}-y$	$\bar{z}$	Si_1	(fgc)	$\frac{1}{2}+x$	$\frac{1}{2}-y$	$\frac{1}{2}+z$

Atoms in special positions

K	(000)	0	y	$\frac{1}{4}$	K	(f00)	0	$\frac{1}{2}+y$	$\frac{1}{4}$
K	(00c)	0	$\bar{y}$	$-\frac{1}{4}$	K	(f0c)	0	$\frac{1}{2}-y$	$-\frac{1}{4}$

Atomic scattering factors were obtained from the empirical curves of Bragg & West (1929) for silicate structures, modified somewhat by the data of Viervoll & Øgrim (1949). These factors were tabulated before the more recent data of MacGillavry *et al.* (1955) were published, and a change to the latter data is difficult and not warranted at this stage. The effective values of the temperature factors were: Al and Si, $B=0{\cdot}3$ Å^2; O, $B=1{\cdot}5$ Å^2; and K, $B=0{\cdot}4$ Å^2. The value of B for potassium is obviously too low, as is shown by the final difference maps. The curves of Bragg & West do not correspond to fully ionised atoms, and since Verhoogen (1958) has suggested that alumino–silicates can be considered as largely ionic the present work would be capable of further refinement by using MacGillavry's data for K^+, Si^{4+}, Al^{3+} and O^{2-}, allowing for anisotropic temp. factors if necessary.

Values of the atomic scattering factors at the points *hkl* (tabulated graphically from the appropriate reciprocal nets) were transferred to punched tape as the input for a structure-factor programme on WREDAC,* for which an additional short tape specified parameters at each cycle. The parameters of Jackson & West were used as a trial structure and refinement proceeded by means of two-dimensional and bounded Fourier and difference syntheses. Bounded projections were partially summed by hand to reduce them to the standard two-dimensional Fourier programme on SILLIAC.†

The major difficulty in the structure analysis of any layer-lattice silicate is the lack of resolution in two-dimensional projections. In the (0kl) projection two of the three crystallographically distinct oxygens in the layer surface (O_D and O_E) are partially superimposed on the Si_1 and Si_2 contours; little improvement was achieved in several refinements. The $h0l$ projection shows Si_1 and Si_2, and O_D and O_E, and O_A, O_B and OH as superimposed, and the x-coordinate of the Al atom is difficult to determine. The $hk0$ projection shows very poor resolution. For these reasons it was necessary to use the following methods.

Bounded Fourier projections

Increased resolution was obtained by using bounded Fourier projections (Lipson & Cochran (1953), p. 80) in which the slabs were $a/2$ and $b/2$ thick (for the projections along [100] and [010]) to restrict the labour of computation. (Only the 0kl, $h0l$, 1kl, 3kl, 5kl and 7kl data were needed to divide the cell into slabs $a/2$ and $b/2$ thick.) Final computations were at 1/128ths of the unit-cell edge; the plane groups of bounded projections differ from those of the two-dimensional projections.

Two cycles of bounded Fourier projections were plotted for the slabs from $a/2$ to a along [100], and $b/2$ to b along [010]. Certain symmetry-related atoms whose centres lie in the slab 0 to $a/2$ project partially into the slab $a/2$ to a, notably the oxygens, which

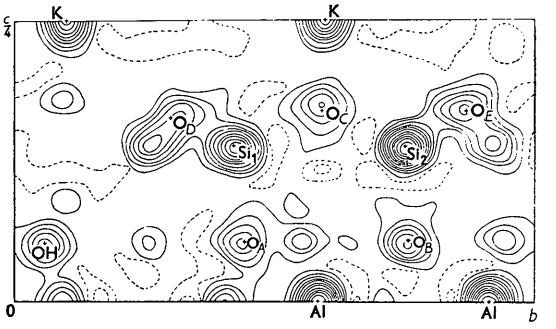

Fig. 2. Bounded Fourier projection along the a-axis for the slab between planes at $x=a/2$ and $x=a$. Contours plotted at intervals of 4 e.Å^{-2}—zero contour broken.

* Complete ordering within $C2/c$ is possible if the unit cell is doubled in size with some kind of disorder present; but no additional reflections indicating this have been observed.

* Weapons Research Establishment Digital Automatic Computer, Salisbury, Sth. Aust. Programme kindly designed and calculations supervised by Mr P. N. L. Goddard and Mr R. Byron-Scott.

† Digital computer, University of Sydney.

have an ionic diameter of 2·8 Å compared with a slab thickness of 2·6 Å. These overlapping atoms do not superimpose on atoms within the slab, except for a portion of an Si_2 atom, which partially masks the O_D atom (Fig. 2). The position of a related Si_2 atom is established elsewhere in the projection, and by subtracting a reasonable fraction of the full electron density from the composite peak fairly circular contours are obtained for O_D.

The overlap of atoms between 0 and $b/2$ into the slab from $b/2$ to b is less but is far more serious since separate x-coordinates cannot be immediately deduced for O_A, O_B and OH (Fig. 4). Furthermore there are two symmetry-related Al atoms, Al(f00) and Al(00c), which superimpose to give a pseudo-centre of symmetry at $x=\frac{3}{4}a$, $z=0$. If Al(000) has coordinates very near $(\frac{1}{4}, y, 0)$ then these composite contour lines are practically circular, and the x and z parameters can hardly be determined. The projection from $3b/4$ to $b/4$ was, however, fairly rapidly calculated from the data for $b/2$ to b, and in this projection Al(000) is completely resolved.

The progress of refinement was followed by calculating $R=\Sigma||F_o|-|F_c||/\Sigma|F_o|$ for the reflections actually observed; after the second cycle of bounded projections this was 0·25. At this stage the bond lengths for the tetrahedral Si_1–O and Si_2–O groups suggested that there may be ordering of the kind $Si_{\frac{1}{2}}Al_{\frac{1}{2}}$ in Si_1 positions and Si in Si_2 positions.

Difference, or (F_o-F_c), syntheses

The parameters of the cations were now sufficiently near their final positions for difference 0kl syntheses to be used to improve the y and z parameters, with much less computation. The R-factor, after four (F_o-F_c) cycles, was 0·12. One $h0l$ difference synthesis was computed, for which the R-factor was 0·19, and it was obvious that the x-parameters of O_AO_B and OH (which are superimposed) needed adjustment. This adjustment could not be made from a difference synthesis of the $hk0$ data which was difficult to interpret because of the direct superposition of O_B on Si_2, and close overlap of O_A, O_C and Si_1.

Most of the interatomic distances and bond lengths were reasonable, except Al–O_A, Al–O_B and Al–OH, but these could be improved by adjusting the x-parameters for O_A, O_B and OH. These could not be easily adjusted otherwise, and nothing is assumed about the tetrahedral bonds by this. At the same time the O–Si–O tetrahedral bond angles all assumed more reasonable values.

Final syntheses

The following projections were computed as the final Fourier syntheses:

(1) A bounded projection along the a-axis, between planes at $x=a/2$ and $x=a$ (Fig. 2).

(2) An (F_o-F_c) two-dimensional projection along the a-axis (Fig. 3).

(3) A bounded projection along the b-axis, between planes at $x=b/2$ and $x=b$ (Fig. 4).

(4) A bounded (F_o-F_c) projection along the b-axis, between planes at $x=b/2$ and $x=b$ (Fig. 5).

Fig. 2 shows all atoms clearly resolved except O_D; the additional unmarked peaks >4e.Å^{-2} are all due to symmetry-related atoms whose centres lie outside the bounds of the slab. The peak heights are quite satisfactorily high, though due to the partial projection of these atoms out of the slab (and also to the somewhat unsatisfactory scattering and temperature factors) the peak values of electron density cannot be discussed in detail. It should be noted that in Fig. 2

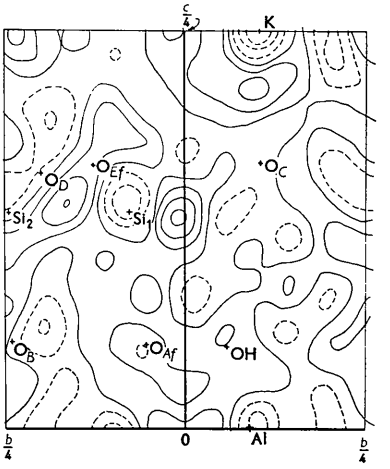

Fig. 3. Two-dimensional (F_o-F_c) map, projected along a-axis. Contours at 1 e.Å^{-2}—negative levels broken.

the centre of the K^+ ion lies in the face of the slab, and therefore the K^+ peak is only at half-height. When Fig. 2 is considered in relation to Fig. 3 it is seen that the K and Al ions are correctly placed but probably need larger temperature factors; that the oxygen atoms are correctly placed, being on flat areas

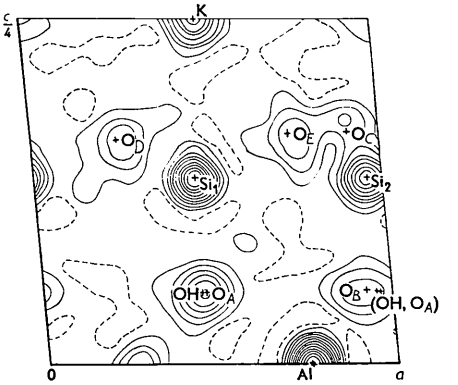

Fig. 4. Bounded Fourier projection along the b-axis for the slab between planes at $y=b/2$ and $y=b$. Contours plotted at intervals of 4 e.Å^{-2}—zero contour broken.

Table 3. *Observed and calculated structure factors*

hkl	F_o	F_c
000	†	+810
2	†	+50
4	89	−70
6	179	+181
8	77	+74
10	237	−229
12	37	+52
14	88	+87
16	129	+126
18	†	+16
20	82	+84
22	101	+89
24	80	+63
26	77	−76
020	41	+23
1	38	+31
2	63	+60
3	119	+106
4	133	+113
5	167	−146
6	18*	−23
7	47	+52
8		+6
9	26	+17
10	37	+31
11	18*	+8
12	36	+34
13	77	−86
14	18*	−10
15	43	+46
16	33	+34
17		−12
18	41	+32
19		+1
20	18*	+36
040	34	−42
1	52	−45
2	71	+61
3	55	+43
4	89	−89
5	18*	−39
6	57	−48
7	41	−44
8	26	−44
9		+16
0,4,10	50	−42
11	60	+52
12	144	−133
13	82	−87
14	44	+43
15	18*	+26
16		−19
17	45	+36
18	37*	−33
19		−26
20		−26
060	275	−258
1	57	+57
2	57	−44
3	18*	+4
4		+14
5	18*	+2
6	57	−65
7	28	−16
8	118	−126
9	60	+51
10	59	+76
11	18*	−33
12	18*	0
13	18*	−8
14	78	−90
15		−11
16	111	−106
17	37	+26
18	18	+32
19	28	−24
20	49	−58
21		+13
22	80	−86
080	18*	−9
1	18*	+3
2	50	−46
3	43	−56
4	18*	−18
5	44	+52
6	18*	−15
7	18*	−8
8	18*	+12
9	18*	−12
10		−12
0,8,11	18*	−21
12		+3
13	64	+75
0,10,0	18*	+9
1		−10
2	27*	−23
3		−3
4	64	+69
5	9*	+23
6	18*	+13
7	9*	+26
8	18*	+35
9		−25
10	37*	+34
11		−4
12	81	+91
110	68	−53
1	47	−38
2	36	−39
3	34	+36
4	161	+137
5	157	−123
6	80	−81
7	10*	+11
8		−11
9	10*	−18
10		−4
11	10*	−21
12	61	+49
13	54	−69
14	55	−67
15	10*	−12
16	9*	−3
17	45	−36
18		−1
19		0
20	32	+29
21	52	−52
22	49	−57
11$\bar{1}$	110	−95
$\bar{2}$		0
$\bar{3}$	110	−105
$\bar{4}$	134	+121
$\bar{5}$	51	+44
11$\bar{6}$	138	−117
$\bar{7}$	62	−77
$\bar{8}$	23	+19
$\bar{9}$	10*	−27
$\bar{10}$	26	+26
$\bar{11}$	49	−35
$\bar{12}$	28	+42
$\bar{13}$	28	+25
$\bar{14}$	59	−58
$\bar{15}$	52	−58
$\bar{16}$	19*	+35
$\bar{17}$	58	−35
$\bar{18}$	10*	+20
$\bar{19}$	29*	−31
$\bar{20}$	29*	+30
$\bar{21}$		+7
$\bar{22}$	38*	−42
$\bar{23}$	48*	−57
130	50	+40
1	191	−212
2	18	+13
3	142	−127
4		−10
5	197	−150
6		+13
7	59	−38
8	31	−18
9	202	−206
10	37	+25
11	109	−68
12		−2
13	67	+56
14		+7
15	69	+20
16		−17
17	141	−150
18		+13
13$\bar{1}$	140	+114
$\bar{2}$	15	+7
$\bar{3}$	143	+109
$\bar{4}$	2	+1
$\bar{5}$	70	−74
$\bar{6}$	30	+21
$\bar{7}$	170	−127
$\bar{8}$	49	−29
13$\bar{9}$	151	+139
$\bar{10}$	15*	+30
$\bar{11}$	197	−183
$\bar{12}$	27	+4
$\bar{13}$	246	−218
$\bar{14}$	24*	−11
$\bar{15}$	60	−32
$\bar{16}$	41	−18
$\bar{17}$	49	+40
$\bar{18}$	44	+25
$\bar{19}$	144	−144
$\bar{20}$		−18
$\bar{21}$	30	−13
$\bar{22}$	27	−3
$\bar{23}$	49	+31
150	38	+40
1	38	−10
2		+14
3	58	−52
4	82	−76
5	61	−53
6	76	+76
7	57	−47
8	10*	−21
9	29*	−26
10	10*	+18
11		−5
12	29*	−45
13		−15
14	29*	+41
15	10*	−17
15$\bar{1}$	38	−25
$\bar{2}$	38	+36
$\bar{3}$	8*	−21
$\bar{4}$	128	−126
$\bar{5}$	38*	+30
$\bar{6}$	81	+79
$\bar{7}$		+5
$\bar{8}$	8*	+1
$\bar{9}$	19*	−50
$\bar{10}$	8*	−36
$\bar{11}$		−18
$\bar{12}$	51	−50
$\bar{13}$	38	−20
$\bar{14}$	77	+76
$\bar{15}$	72	−48
$\bar{16}$		−40
1,5,$\bar{17}$	19*	−33
$\bar{18}$	10*	−12
$\bar{19}$	10*	−5
170	30	+31
1	41	+46
2	14*	+27
3	105	−84
4	79	−83
5	77	+83
6	10*	+23
7		−5
8	19*	+54
9	29*	−13
10	14*	−25
11		+15
12	10*	−19
13	106	+108
14	38*	+53
17$\bar{1}$	116	+92
$\bar{2}$	38	−45
$\bar{3}$	82	+84
$\bar{4}$	10*	−18
$\bar{5}$		−2
$\bar{6}$	38*	+46
$\bar{7}$	93	+101
$\bar{8}$		−7
$\bar{9}$		0
$\bar{10}$		−3
$\bar{11}$		+27
$\bar{12}$		−15
$\bar{13}$	29	−35
190	60	+53
1	66	+85
2		−11
3	106	+107
4	14*	0
5		+2
6		−24
7		−16
8	19*	+45
9	115*	+137

Table 3 (*cont.*)

hkl	F_o	F_c
10	10*	−38
11	14*	+38
12	10*	−8
191	67*	−55
2	29*	−28
19$\bar{3}$	14*	−28
$\bar{4}$	10*	+1
$\bar{5}$	68	+83
$\bar{6}$		−14
$\bar{7}$	38*	+47
$\bar{8}$	38*	+39
$\bar{9}$	10*	−30
$\bar{10}$	24*	−45
$\bar{11}$	57	+68
$\bar{12}$		+5
$\bar{13}$	77	+86
310	†	−15
1	29	−27
2	85	−87
3	82	+96
4	117	+112
5	22	+7
6	10*	−14
7	15	+8
8	38	−31
9	35	+47
10		+3
11	90	+79
12	65	+65
13		−22
14	46	−49
15	31	+35
16		+6
17	48	+26
31$\bar{1}$	†	−10
$\bar{2}$	35	+27
$\bar{3}$	80	+40
$\bar{4}$	29	+24
$\bar{5}$	124	+83
$\bar{6}$	78	−86
$\bar{7}$		+2
$\bar{8}$	35	+35
$\bar{9}$	60	+57
$\bar{10}$		−7
$\bar{11}$	31*	+24
$\bar{12}$	31*	+24
$\bar{13}$	15*	+52
$\bar{14}$	59	−57
$\bar{15}$	31*	−15
$\bar{16}$		+15
$\bar{17}$	15*	+17
$\bar{18}$	21*	+5
3,1,$\bar{19}$		+16
$\bar{20}$		−1
$\bar{21}$	15*	+41
$\bar{22}$	60	−60
330	32	−21
1	73	+45
2		+0
3	10*	−23
4		−10
5	46	+38
6	31	+22
7	153	+126
8	36	−24

hkl	F_o	F_c
9	89	−91
10		+7
11	42	−2
12	40	+12
13	95	+100
14		+6
15	135	+122
16	41*	−24
17	31*	−34
18	10*	+18
19	67	+70
20		−5
21	92	+81
33$\bar{1}$	263	+281
$\bar{2}$	38	+7
$\bar{3}$	54	+53
$\bar{4}$		−1
$\bar{5}$		−10
$\bar{6}$	10*	+5
$\bar{7}$	67	+73
$\bar{8}$		−13
$\bar{9}$	146	+132
$\bar{10}$	31	+29
$\bar{11}$	96	−101
$\bar{12}$	15*	−14
$\bar{13}$	15*	−4
$\bar{14}$		−3
$\bar{15}$	106	+84
$\bar{16}$		−4
$\bar{17}$	122	−102
$\bar{18}$		+13
$\bar{19}$	20*	−33
$\bar{20}$		−14
$\bar{21}$	74	+73
3,3,$\bar{22}$		+7
$\bar{23}$	89	+84
$\bar{24}$		−3
$\bar{25}$	40	+40
350		+2
1		+17
2	99	+101
3	31*	+35
4	121	−106
5	10*	−12
6		+18
7	31*	−18
8	59	+44
9	10*	+28
10		−5
11	31*	+20
12	56	−73
13	43	+16
14	61	+55
15	36*	+26
16	10*	−19
17	26*	+28
18		−4
35$\bar{1}$	46	+8
$\bar{2}$	57	−43
$\bar{3}$	108	+66
$\bar{4}$		−17
$\bar{5}$	71	+50
$\bar{6}$	78	+75
$\bar{7}$	31*	+17
$\bar{8}$	52	−57
$\bar{9}$	31*	+16
$\bar{10}$	10*	+26

hkl	F_o	F_c
$\bar{11}$		+11
$\bar{12}$		−16
$\bar{13}$		−3
$\bar{14}$	31*	+47
370	10*	+18
1	10*	+14
2		+8
3	78	−84
4	21*	−34
5		−7
6		−9
377	15*	−49
8		+11
9	46*	−34
10		+12
11	95	−80
12	31*	−31
37$\bar{1}$		+7
$\bar{2}$		+2
$\bar{3}$		+21
$\bar{4}$	46	−26
$\bar{5}$	94	−75
$\bar{6}$	31*	+43
$\bar{7}$		+3
$\bar{8}$		+22
$\bar{9}$		−39
$\bar{10}$		−31
$\bar{11}$	66	−40
$\bar{12}$		−9
$\bar{13}$	82	−87
$\bar{14}$	31*	+45
$\bar{15}$	31*	+25
390	31*	+42
1	15*	−10
2		−11
3	15*	−9
4		+9
5	15*	−38
6	15*	−26
7	75	−82
8	31*	+36
9		+9
10		−15
39$\bar{1}$	97	−116
$\bar{2}$	31*	−34
$\bar{3}$	46*	−43
$\bar{4}$	20*	−4
$\bar{5}$	31*	+28
$\bar{6}$	31*	−2
$\bar{7}$		−37
$\bar{8}$	46*	+29
$\bar{9}$	120	−112
$\bar{10}$	61*	−53
510	14*	−27
1	10*	−15
2	36	+46
3	25	−16
4	25	−30
5	15*	−14
6	10*	−4
7	59	−40
8		+0
9	70	−29
10	47	+48

hkl	F_o	F_c
11		−1
12	41	−52
51$\bar{1}$	†	−19
$\bar{2}$	†	+3
$\bar{3}$	†	−14
$\bar{4}$	†	+21
$\bar{5}$	†	+20
$\bar{6}$	44	−43
$\bar{7}$	50	−45
$\bar{8}$	10*	+30
$\bar{9}$	14	−15
$\bar{10}$	14*	+17
$\bar{11}$	44	−23
$\bar{12}$	10*	+23
$\bar{13}$	14*	−6
$\bar{14}$	48*	−44
$\bar{15}$	58*	−63
530	10*	−21
1	30	−25
2		+5
3	70	−62
4		−2
5	74	−71
6	10*	+6
7	36	+32
8	10*	−10
9	58	−86
10		+8
11	109	−97
12		−6
13	61	−43
14		+14
15	53	+52
16		−11
17	65	−80
18		+1
53$\bar{1}$	64	+84
$\bar{2}$	20	+21
$\bar{3}$	88	−90
$\bar{4}$		−2
$\bar{5}$	99	−95
$\bar{6}$		−6
$\bar{7}$		−18
$\bar{8}$		−5
$\bar{9}$	10*	+11
$\bar{10}$	14*	+20
$\bar{11}$	147	−166
$\bar{12}$		−17
$\bar{13}$	41	−32
$\bar{14}$		+0
$\bar{15}$	43	+30
$\bar{16}$		−1
550	14*	−27
1	10*	−15
2	36	+46
3	25	−16
4	25	−30
5	15*	−14
6	10*	−4
7	59	−40
8		+0
9	70	−29
10	47	+48
11		−1
12	41	−52
55$\bar{1}$	24*	−2

Table 3 (*cont.*)

hkl	F_o	F_c
$\bar{2}$	†	+5
$\bar{3}$	30	+6
$\bar{4}$	27	−28
$\bar{5}$	10*	+1
$\bar{6}$	40	+44
$\bar{7}$	39	−17
$\bar{8}$		−18
$\bar{9}$	34	−33
$\bar{10}$		−14
$\bar{11}$	47	−17
$\bar{12}$	20	−22
$\bar{13}$	66	−23
$\bar{14}$	60	+56
$\bar{15}$	46	−36
$\bar{16}$	34	−52
570		+6
1	78	+80
2	39	+28
3	43	−28
4	39*	−34
5	19*	+39
6	14*	−17
7	52	+26
8	19*	+21
$57\bar{1}$	39*	+35
$\bar{2}$	19*	−26
$\bar{3}$		+21
$\bar{4}$		+6
$\bar{5}$		−12
$\bar{6}$	39*	+29
$\bar{7}$	64	+57

hkl	F_o	F_c
590	29*	+30
1	19*	+14
2		−1
$59\bar{1}$	39*	−43
$\bar{2}$	58*	−42
$\bar{3}$	92	+85
$\bar{4}$		+13
$\bar{5}$	69	+59
730		−3
1	68	+65
2		−3
3		+5
4		−6
5		−4
6		+16
7	74	+93
$73\bar{1}$	90	+96
$\bar{2}$		+14
$\bar{3}$	42	−56
$\bar{4}$		−12
$\bar{5}$		+25
$\bar{6}$		+4
$\bar{7}$	78	+65
$\bar{8}$		−1
$\bar{9}$		+24
$\bar{10}$		+9
7,3,$\bar{11}$	43	−48
$\bar{12}$		−11
$\bar{13}$	57	+73
$\bar{14}$		+6
$\bar{15}$	45	+49

hkl	F_o	F_c
200	119	
2	123	+116
4	56	−75
6	140	−146
8	125	+111
10	161	−192
12	224	−211
14	73	−43
16	56	+56
18	95	−129
20	30*	−15
22	47	+31
24	40	+11
26	88	−103
$20\bar{2}$	194	−190
$\bar{4}$	119	−100
$\bar{6}$	181	−161
$\bar{8}$	70	−64
$\bar{10}$	218	−222
$\bar{12}$	98	−89
$\bar{14}$	52	+45
$\bar{16}$	73	+51
$\bar{18}$	142	−150
$\bar{20}$		+31
$\bar{22}$	45	+20
$\bar{24}$	83	−88
400	153	+186
2	123	+137
4	10*	+33
6	20*	+25
8	153	+175

hkl	F_o	F_c
10	20*	+3
12	10*	−30
14		−7
16	80	+101
$40\bar{2}$	122	−121
$\bar{4}$		+7
$\bar{6}$	117	+98
$\bar{8}$	46	+35
$\bar{10}$	83	−88
$\bar{12}$	142	+142
$\bar{14}$	128	+119
$\bar{16}$	47	+42
$\bar{18}$	10*	−18
$\bar{20}$	95	+106
$\bar{22}$	41	+25
$\bar{24}$	10*	−17
600	52	−43
2	47	+30
4		−8
6	117	−119
8	30*	+57
10	10*	+3
12	73	−84
$60\bar{2}$	115	−141
$\bar{4}$		−7
$\bar{6}$	20*	−35
$\bar{8}$	47	−36
$\bar{10}$	83	−90
$\bar{12}$		+33
$\bar{14}$	10*	+9
$\bar{16}$	33	−45

* These reflections are visually estimated since they are too weak for satisfactory measurement.
† These reflections were not photographed.

of Fig. 3; and that Si_1 (and possibly Si_2) need a shift of $<0{\cdot}012$ Å (apparently in the $+\delta y$ and $-\delta z$ direction) together with some adjustment of the temperature factor.

Fig. 4 does not completely resolve the octahedral oxygens, nor does it separate two related octahedral Al ions which are practically superimposed in this projection. These Al ions and the K ion are only partly within this slab, and symmetry related atoms to O_A and OH partly project on to O_B. All unlabelled peaks >4 e.Å^{-2} are due to atoms whose centres lie outside the slab. The peaks of the atoms are satisfactorily high, except for Si_2 which is sharp but shows a low peak electron density.

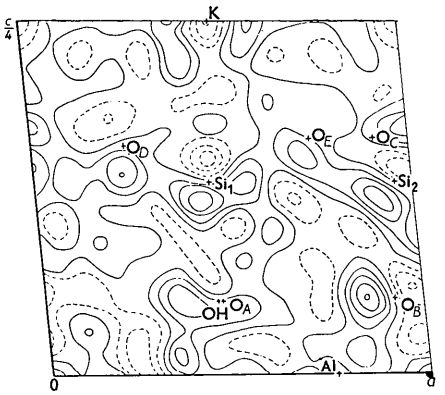

Fig. 5. Bounded (F_o-F_c) map, projected along b-axis for the slab between planes at $y=b/2$ and $y=b$. Contours plotted at intervals of 1 e.Å^{-2}—negative levels broken.

Fig. 5, on a scale of 1 e.Å^{-2}, suggests that very small adjustments in certain parameters may help further. In particular it had not been possible from any previous map—either the bounded electron-density or the $h0l$ difference map—to determine which x-parameters for O_A, O_B and OH needed adjustment. Fig. 5, however, shows quite clearly that (O_A+OH) lie on a flat part of this (F_o-F_c) map; and they cannot therefore contribute at all (through the *partly* protruding symmetry related atoms) to the *difference* density in the region of O_B. The bounded difference map therefore suggests that the x-coordinate for O_B should be reduced by about 0·04 Å. The tetrahedral oxygens appear to be correctly placed, but Si_1 and Si_2 may require small shifts (of $<0{\cdot}012$ Å along slope).

Results

The observed and the calculated structure factors (F_o and F_c) suitably scaled, are given in Table 3,

Table 4. *Initial and final atomic parameters*

(as decimal fractions of unit-cell dimensions)

	Jackson & West			Final coordinates			Shift (Å)		
Atom	x	y	z	x	y	z	$\|\delta x\|$	$\|\delta y\|$	$\|\delta z\|$
Al(000)	250	083	000	2484	0871	0016	0·008	0·036	0·032
O_A(000)	438	917	055	4650	9450	0527	0·140	0·252	0·046
O_B(000)	438	250	055	4250	2600	0542	0·016	0·090	0·016
OH(000)	438	583	058	4530	5580	0520	0·078	0·225	0·120
Si_1(000)	467	917	135	4625	9242	1372	0·023	0·065	0·044
Si_2(000)	467	250	135	4593	2550	1365	0·040	0·045	0·030
O_C(000)	480	083	164	4080	0960	1680	0·374	0·117	0·080
O_D(000)	228	833	164	2450	8020	1620	0·088	0·279	0·040
O_E(000)	228	333	164	2629	3713	1674	0·181	0·344	0·068
K(000)	000	083	250	0000	1016	2500	0	0·167	0

from which it is seen that these agree satisfactorily. The R-factors (measured intensities only) have the following values: $R(0kl)=0{\cdot}12$; $R(h0l)=0{\cdot}13$; R (all measured reflections) $=0{\cdot}17$.

The final values of the atomic parameters, together with the 'ideal' parameters, are given in Table 4, and the bond lengths, interatomic distances and bond angles are recorded in Table 5. The Si_1–O bond lengths (mean $=1{\cdot}69_5$ Å) are clearly different from the Si_2–O bonds (mean $=1{\cdot}61_2$ Å); and within each tetrahedron the bond to the apical oxygen, within the layer, is rather larger than the others. The difference is possibly significant for Si_2–O_B (where $\delta l/\sigma=2{\cdot}2$) and may reflect the different coordination and therefore different ionic radius of the apical oxygens. The K–O bonds also clearly fall into two groups of three, the average K–O distance for one group being $2{\cdot}81_2$ Å, and for the remainder $3{\cdot}39_0$ Å; the symmetry operations bring the total oxygen group around the K^+ to 12. For the O–O interatomic distances (fixed by packing) around the tetrahedral groups the six distances around Si_1 are close to the mean value, $2{\cdot}76_9$ Å, as are the O–O distances from the apical oxygen to the three basal oxygens around Si_2. The three O–O distances in the base of the Si_2 group, however, have values very close to their mean, $2{\cdot}58_7$; and the corre-

Table 5. *Bond lengths, interatomic distances and bond angles*

(1) Tetrahedral groups

Si_1–O_C	$1{\cdot}69_5$ Å	Si_2–O_C	$1{\cdot}59_6$ Å
Si_1–O_D	$1{\cdot}68_2$	Si_2–O_D	$1{\cdot}58_1$
Si_1–O_E	$1{\cdot}68_9$	Si_2–O_E	$1{\cdot}62_3$
(Mean $=1{\cdot}69_0$)		(Mean $=1{\cdot}60_0$)	
Si_1–O_A*	$1{\cdot}71_0$	Si_2–O_B*	$1{\cdot}64_8$
Mean $=1{\cdot}69_5$ Å		Mean $=1{\cdot}61_2$ Å	

* Apical oxygens.

Around Si_1

O_C–O_D	$2{\cdot}77_5$ Å	O_A*–O_C	$2{\cdot}74_3$ Å
O_C–O_E	$2{\cdot}73_3$	O_A*–O_D	$2{\cdot}87_0$
O_D–O_E	$2{\cdot}74_9$	O_A*–O_E	$2{\cdot}74_1$
Mean $=2{\cdot}76_9$ Å			

* Apical oxygens.

Around Si_2

O_C–O_D	$2{\cdot}58_3$ Å	O_B*–O_C	$2{\cdot}74_3$ Å
O_C–O_E	$2{\cdot}58_8$	O_B*–O_D	$2{\cdot}80_6$
O_D–O_E	$2{\cdot}59_1$	O_B*–O_E	$2{\cdot}73_2$
(Mean $=2{\cdot}58_7$)		(Mean $=2{\cdot}76_0$)	
Mean $=2{\cdot}67_4$ Å			

* Apical oxygens.

O_C–Si_1–O_D	110° 24′	O_A–Si_1–O_C	106° 16′
O_C–Si_1–O_E	108° 15′	O_A–Si_1–O_D	115° 33′
O_D–Si_1–O_E	111° 52′	O_A–Si_1–O_E	107° 22′
Mean $=109°\ 58'$			

O_C–Si_2–O_D	107° 14′	O_B–Si_2–O_C	114° 35′
O_C–Si_2–O_E	107° 3′	O_B–Si_2–O_D	109° 8′
O_D–Si_2–O_E	107° 49′	O_B–Si_2–O_E	109° 32′
(Mean $=107°\ 22'$)			
Mean $=109°\ 13'$			

Table 5 (*cont.*)

Si_1–O_C–Si_2	129° 22′	Si_1–O_D–Si_2	135° 24′
Si_1–O_E–Si_2	128° 42′		
Mean $=131°\ 9'$			

(2) Octahedral groups

Al–O_A	$1{\cdot}93_5$ Å	Al–O_A	$1{\cdot}94_4$ Å
Al–O_B	$1{\cdot}93_2$	Al–O_B	$2{\cdot}04_8$
Al–OH	$1{\cdot}93_9$	Al–OH	$1{\cdot}93_0$
Mean $=1{\cdot}95_4$ Å			

Around Al

O_A–O_A	$2{\cdot}39_6$ Å*	OH–O_A	$2{\cdot}73_1$ Å
O_A–O_B	$2{\cdot}90_9$	OH–O_B	$2{\cdot}80_7$
O_A–O_B	$2{\cdot}92_6$	OH–O_B	$3{\cdot}04_6$
O_A–O_B	$2{\cdot}84_1$	OH–O_B	$2{\cdot}68_4$
O_A–OH	$2{\cdot}73_4$	OH–OH	$2{\cdot}51_1$*
O_A–OH	$2{\cdot}88_1$	O_B–O_B	$2{\cdot}76_8$*
Mean $=2{\cdot}76_9$ Å			

* These oxygen–oxygen distances correspond to shared edges of neighbouring octahedra.

(3) Interlayer cation

K–O_C	$2{\cdot}79_9$ Å	K–O_C	$3{\cdot}35_7$ Å
K–O_D	$2{\cdot}77_5$	K–O_D	$3{\cdot}51_1$
K–O_E	$2{\cdot}86_2$	K–O_E	$3{\cdot}30_3$
Mean $=2{\cdot}81_2$ Å		Mean $=3{\cdot}39_0$ Å	

sponding bond angles are consistent with this. There is more variation in the interatomic O–O and O–OH distances in the octahedral configuration around the Al atom. The mean, $2{\cdot}76_9$ Å, is close to the oxygen diameter; one O–O distance is rather small (2·40 Å). The O–Si–O angles are all close to the tetrahedral angle of 109° 28′.

Accuracy

The accuracy of the positional parameters and certain bond lengths determined in this analysis has been computed as recommended by Lipson & Cochran (1953), using the final ϱ_0 bounded projections and the a-axis $(F_o - F_c)$ projection. The standard deviations of these bond-lengths have been used to determine the significance of bond length differences between the two silicon tetrahedral groups, as suggested by Cruickshank (1949). The standard deviations $\sigma(x_n)$ have been computed over the whole unit cell, which is a slight over-estimate of error; computational errors are not allowed for. Since there is little evidence of asymmetry (except possibly for the K atom) the standard deviations have been assumed equal in all directions. The values of the curvatures and $\sigma(x_n)$ are given in Table 6, together with the standard deviations of bond lengths and mean bond lengths. The significance test shows that the bond lengths in the two silicon tetrahedra are significantly different; and the standard deviations of the mean Si_1–O and Si_2–O bond lengths are consistent with the hypothesis that Si_2 is fully occupied by silicon, whilst Si_1 is occupied by $Si_{\frac{1}{2}}Al_{\frac{1}{2}}$, within the limits of Smith's (1954) curve.

Table 6. *Accuracy of atomic parameters and bond lengths*

	p	$-C_n$ (e.Å^{-4})	$\sigma(x)$ (Å)
K	7·0	1036	0·0048 Å
Al	7·7	740	0·0067
Si_1	7·5	585	0·0085
Si_2	7·5	720	0·0069
O_A	6·5	260	0·0192
O_B	6·0	288	0·0173
O_C	4·5	171	0·0292
O_D	7·0	294	0·0170
O_E	5·5	264	0·0189
OH	6·5	300	0·0166

Mean $\sigma(x)$ for oxygens = 0·0197 Å
$\sigma(\varrho)$ over whole unit cell = 1·15 e.Å^{-2}

Bond lengths

$\sigma(Si_1–O_C)$	= 0·030 Å	$\sigma(Si_2–O_C)$	= 0·030 Å
$\sigma(Si_1–O_D)$	= 0·019	$\sigma(Si_2–O_D)$	= 0·018
$\sigma(Si_1–O_E)$	= 0·021	$\sigma(Si_2–O_E)$	= 0·020
$\sigma(Si_1–O_A)$	= 0·021	$\sigma(Si_2–O_B)$	= 0·019
Mean $\sigma(Si_1–O)$	= 0·023 Å	Mean $\sigma(Si_2–O)$	= 0·022 Å
Mean $\sigma(Al–O)$	= 0·019 Å	Mean $\sigma(K–O)$	= 0·020 Å
Mean $\sigma(O–O)$	= 0·028 Å		

Standard deviations of mean bond lengths

σ(mean Si_1–O)	= 0·012 Å	σ(mean Si_2–O)	= 0·011 Å
σ(mean Al–O)	= 0·012 Å	σ(mean O–O) around Si_1	= 0·011 Å

For the difference between the mean Si_1–O and mean Si_2–O bond lengths
$\delta l/\sigma = 5{\cdot}19$ (highly significant)

For the difference between the mean Si_1–O and $Si_{\frac{1}{2}}Al_{\frac{1}{2}}$–O = $1{\cdot}69 \pm 0{\cdot}015$
$\delta l/\sigma = 0{\cdot}20$ (not significant)

For the difference between the mean Si_2–O and Si–O = $1{\cdot}60 \pm 0{\cdot}01$
$\delta l/\sigma = 0{\cdot}54$ (not significant)

For the difference between the mean Si_2–O = $1{\cdot}60_0$ and Si_2–O_B = $1{\cdot}64_8$
$\delta l/\sigma = 2{\cdot}22$ (possibly significant)

Discussion

The present analysis has yielded new atomic parameters which depart significantly from the 'ideal' coordinates of Jackson & West (1931, 1933). Certain of these 'distortions' appear to be a common feature of the layer-lattice silicates, and will be discussed in the next section in relation to other recently published structures. Some of the difficulties of the ideal muscovite structure can now be resolved as follows.

(*a*) *Forbidden reflections*

Reflections of the kind 06l, l odd are no longer forbidden since the actual y parameters in muscovite are not multiples of $b/12$ (Table 4). The departures from ideal parameters account for the observed intensities.

(*b*) *Monoclinic angle*

The monoclinic angle for the various layer silicates can be predicted theoretically by considering the packing of the octahedral O and OH sheets, together with the packing of the O and OH surface layers in minerals such as the kaolins (Brindley, 1951). The monoclinic angle for a number of idealized structures is given by $\beta = \cos^{-1}(-a/3c)$, even though the number of layers and their type varies from structure to structure. The $-a/3$ shift for $1M$ muscovite is across the octahedral layer, the surface layers packing together without stagger. For the ideal $2M_1$ muscovite each octahedral layer shows a shift of $-a/3$, but this is now at $\pm 60°$ to the a-axis—a net shift of $-a/3$, so that $\beta = 94°\ 55'$ theoretically. Direct superposition of one layer on the next is assumed, the K^+ ions being symmetrically placed in the hexagonal 'holes' in the oxygen surface sheet.

A diagrammatic projection normal to the a–b plane clearly shows that this is not so. The K^+ ion is no longer at the geometric centre of the oxygen network, but is displaced from it, towards the unfilled octahedral sites above and below the K^+ ion; this displacement from the geometric centre of the oxygens is in the reverse direction on the opposite side of the 10 Å layer.

If we assume that $\beta = 95° 11'$ then the interlayer K–K vectors (Smith & Yoder, 1956) are at $\pm 63° 36'$ to the a-axis, rather than $\pm 60°$. The displacement of the K^+ ion from the geometric centre of the oxygens is largely the reason for the departure of β from the theoretical value. Ideally the K–K vector has a length in normal projection of $a/3 = 1{\cdot}72$ Å; and if all the layer stagger occurs in the octahedral layer then certain Si–Si vectors, in normal projection, will also be 1·72 Å. The observed values are 1·85 Å for the appropriate Si–Si vectors, but 2·04 Å for the K–K vector, which confirms that the O–K–O sheets (as well as the octahedral layers) contribute to the observed monoclinic angle.

(c) *Distortion and tilt of surface oxygen network from hexagonal*

In the ideal triphormic layer silicate structures the surface of each layer consists of an open hexagonal network of basal oxygen atoms of the Si–O tetrahedra. In several structures examined recently this hexagonal network has been shown to be distorted, usually to an approximately ditrigonal configuration, as in crocidolite (Whittaker, 1949), Mg-vermiculite (Mathieson & Walker, 1954), dickite (Newnham & Brindley, 1956), amesite (Steinfink & Brunton, 1956) and prochlorite (Steinfink, 1958*a*). Mathieson & Walker described the distortion in vermiculite as the net effect of rotations of whole Si–O tetrahedra of about $\pm 5\frac{1}{2}°$. A similar distortion is evident in muscovite, but appears to be greater than for the minerals previously examined, since the basal triads in muscovite have rotated about 13° from the ideal positions, compared with 4°–6° for other minerals. The six oxygens of any hexagon are now at the corners of two interpenetrating triangles which are approx. equilateral and coplanar, with sides 3·9 Å and 5·1 Å respectively. The surfaces thus have a marked ditrigonal rather than hexagonal symmetry. The octahedral layer is less distorted from the ideal hexagonal packing; 'shared edges' of octahedra are shortened in conformity with Pauling's Rules.

Several hypotheses have been advanced to account for this apparently characteristic distortion of the hexagonal layer-lattice silicate surface. Mathieson & Walker (1954) suggested the presence of residual charges on surface oxygens and octahedral cations which, if present, would produce a torque in the right direction. Whittaker (1956) pointed out that this explanation cannot apply to clino-chrysotile, due to the distortion alternating in direction in this two-layer structure. Newnham & Brindley (1956) explain the distortion in dickite as due to the considerable misfit between the tetrahedral and octahedral layers. Bradley (1957) has discussed the possible relationships (for layer silicates) between the 'free' dimensions of the tetrahedral and octahedral layers, the decrease in these dimensions achieved either by ordering or by the rotation of the tetrahedral groups through small angles, and the thickness of the octahedral layer in relation to the strain imposed on it.

In the case of the micas the distortions in the oxygen network are apparently primarily due to misfit between the tetrahedral and octahedral layers. Brindley & MacEwan (1953) have proposed formulae for calculating the b-axes of 'free' tetrahedral and octahedral layers with various cationic substitutions. (The b-dimension only need be considered since $a = b/\sqrt{3}$ very nearly.) For a tetrahedral layer with all sites occupied by Si the b-axis is about 9·10 Å, but for a net with Si:Al = 3:1 the b-axis is about 9·27 Å ($9{\cdot}30 \pm 0{\cdot}06$, Smith & Yoder, 1956). The gibbsite, $Al(OH)_3$, b-axis is 8·64 Å. In muscovite* ($b = 8{\cdot}995$ Å) there must be a considerable contraction of the tetrahedral layer to fit the octahedral layer, which must be correspondingly stretched. Bradley (1957) has pointed out that a stretched octahedral layer probably reduces in thickness; for gibbsite the layer thickness is 2·53 Å, but the octahedral layer in muscovite is approximately 2·12 Å thick.

A rotation of the tetrahedra of about 13°—which is quite feasible—allows the necessary contraction of the silicate layer. This fitting together of different sized layers does not, however, dictate the *direction* in which any given tetrahedra will rotate. It may be that small residual charges on the surface oxygens and octahedral aluminiums govern the direction of rotation. (Such attractive forces would, it is to be noted, initiate rotations in the directions observed).

The parameters (Table 4) show that the Si–O tetrahedra in muscovite are slightly tilted, this being seen more readily in a normal projection on to the a–b face. The tilt of the triad of basal oxygens is matched by the displacement of the apical oxygens, O_A and O_B from vertically below Si_1 and Si_2 respectively. The oxygen O_A (and O_B) is ideally sited equidistant from three possible octahedral cation positions. The displacement of O_A (and of O_B) is away from the unoccupied, and towards the two occupied Al sites, as expected. Gatineau & Mering (1958) in a one-dimensional structural analysis of muscovite (using 27 00l terms(!)) proposed a 'static disorder of the oxygen network in the c-direction'. It would appear that for such data the effect of temperature and statistical disorder would be difficult to differentiate. The present parameters do not agree with their data, nor does their hypothesis of complete ordering of 3 Si and 1 Al fit the accepted space group, $C2/c$.

(d) *Oxygen configuration around interlayer cation*

In the ideal muscovite structure the K^+ ion is in 12-coordination with equidistant oxygens, six above and six (symmetry-related) below the K^+ plane. In the real structure the K^+ is still on a two-fold axis, but the six independent oxygens are no longer equi-

* For $2M_1$ muscovite the b-axis of the separate 10 Å layers is still 8·995 Å approx.

distant (Fig. 6). Fig. 6 also clearly shows the K^+ ion to be closely surrounded by six oxygens at an average distance of 2·81$_2$ Å, and then by an outer shell of six, at a mean distance of 3·39$_0$ Å. Since the sum of the ionic radii for K^+ and O^- in 12-coordination is about 2·95 Å it is clear that the six inner oxygens (three above, interleaved with three below) must be in close contact with the K^+ ion—indeed a bond of 2·81 Å suggests a lower K^+ coordination than 12. These surface oxygens appear to be so displaced from hexagonal symmetry by the strains in the structure that the 'hole' left for the K^+ is too small for this ion to fit into completely. It therefore holds the layers slightly apart, and this is confirmed by the interatomic distance between two oxygens (across the K^+ layer) being 3·4 Å, whereas the expected O–O distance is approximately 2·8 Å.

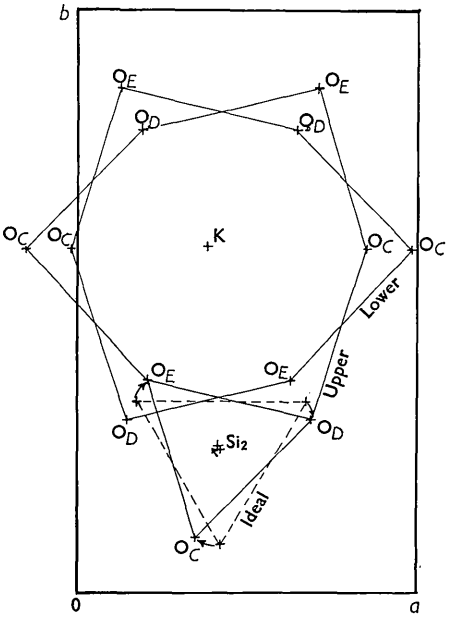

Fig. 6. *Normal* projection on to the *a*–*b* face of some of the atoms in muscovite. This clearly shows the di-trigonal character of the oxygen network, the inner ring of six oxygens around K^+, and the rotation of the tetrahedra from the ideal structure.

The six outer oxygens around the K^+ are still at reasonable distances, except possibly the pair at 3·51 Å away from the K^+ ion; the latter may have little effective bonding to the K^+.

(e) Silicon–aluminium ordering

Ordering of Si and Al atoms—either partial or complete—in tetrahedral 'Si' sites has been observed recently for a number of silicate structures (e.g. felspars). Ordering is usually established by a comparison of observed bondlengths with the data, summarized by Smith (1954), showing the essentially linear increase in 'Si'–O bondlength as the average Al occupancy of the tetrahedral sites is increased. For the pure Si–O bond the distance is close to 1·60 Å; the Al–O bondlength is rather less well-established as 1·78 Å. The bondlengths in muscovite (Table 5) show that the tetrahedral positions are partially ordered, the 'Si_2' sites being almost fully occupied by Si atoms, and the 'Si_1' positions by $Si_{\frac{1}{2}}Al_{\frac{1}{2}}$ atoms on the average. The Si_2–O_B bond (Table 2) may be larger than 1·60 Å because O_B is an apical oxygen, whereas the short O–O distance in the Si_2 tetrahedral base reflects the Si occupancy of this site. This is the maximum ordering possible within the space group ($C2/c$) requirements, and no evidence of lower symmetry—allowing higher ordering—has been found. Further ordering would no doubt cause sufficient displacements of the oxygen atoms to give additional reflections. Nevertheless the result is a little surprising in view of the number of reliable muscovite analyses in which there are exactly three Si and three Al atoms per unit cell; complete ordering might be expected as a possible structural mechanism to ensure this exact 3:1 ratio of Si to Al tetrahedrally.

A satisfying explanation of the ordering of Si and Al in these structures has not been found. Since the tetrahedral cations all have equivalent octahedral configurations in their neighbourhood ordering can hardly be due to muscovite being dioctahedral. It appears, however, that one, or possibly two, oxygens in any surface hexagon are sufficiently distant from the K^+ ion (3·51 Å, and 3·36 Å) to give some local lack of charge balance. Though this may aid any ordering process it is difficult to see how such charge unbalance could *cause* the trigonal symmetry shown by the alternation of Si and $Si_{\frac{1}{2}}Al_{\frac{1}{2}}$ sites around the hexagons.

(f) Polymorphism of muscovite

Polymorphism in the micas arises because an $a/3$ stagger in the octahedral region of each 10 Å layer is combined with the (ideal) hexagonal symmetry of the surface oxygen network. Smith & Yoder (1956), in a discussion of mica polymorphism both theoretically and experimentally, predicted that six simple polymorphs should be observed. For muscovite only the $1M$, $2M_1$, and (less commonly) 3T polymorphs have been found; but the $2M_2$ polymorph has also been observed (for lepidolites) though 20 and 6H micas have yet to be found. Radoslovich (1959) has suggested that the reason for this lies in the trigonal rather than hexagonal symmetry of the actual layer surfaces of micas. Such surfaces can fit together most readily in ways which correspond to no rotation, or to rotations which are multiples of 120°, between layers. Those polymorphs which correspond to rotations between layers which are multiples of 60° (2O, $2M_2$ and 6H) should only be observed in micas showing little or no distortion of the oxygen network.

This hypothesis—if substantiated by several structural analyses—explains the abundance of the $1M_1$,

$2M_1$ and 3T micas, but does not suggest why 3T occurs less frequently than $2M_1$, to which it is converted at high temperature (Smith & Yoder, 1956). For the following discussion of a possible 'mechanism' of structural control it is assumed that

(i) the trigonal symmetry precludes 180° rotations between layers;
(ii) the K^+ ion is displaced from the centre of the oxygen network by some small force;
(iii) the two potassium ions on opposite sides of one layer tend to move as far apart as possible.

Now suppose that K_1^+ at the top of layer A is acted on by a small force in one direction (away from O_D?) within its surrounding oxygen network. In the $1M$ structure the same K_1^+ experiences an opposing force from the bottom of layer B (Fig. 7(*a*)). A more stable state may be reached, however, if these two forces act as nearly as possible in the same direction. The nearest permissible approach to this, because of the trigonal symmetry, is at 60° to each other; and the resultant force on K_1^+ will lie between the two (Fig. 7(*b*)). The force on K_2^+ at the top of layer B is

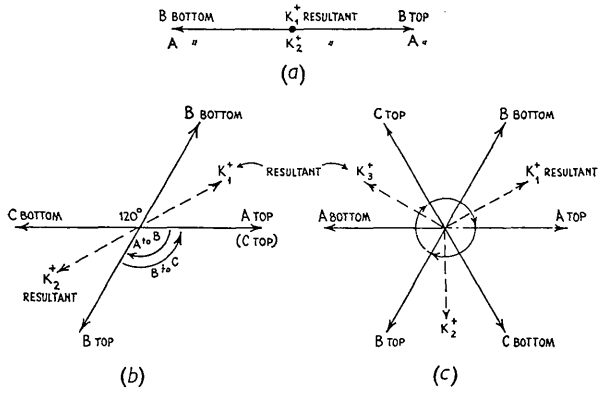

Fig. 7. (*a*) Forces on the K^+ ions in the $1M$ structure, from successive layers A and B. (*b*) Forces on the K^+ ions in the $2M_1$ structure, from successive layers A, B and C. (*c*) ditto in $3T$ structure.

then at 120° to that on K_1^+ at the top of layer A. If layer C also rotates relative to B (to likewise reach a more stable position) then this rotation may be either a further +120°, or else −120°. Of these the latter results in a net force on, and displacement of, K_2^+ which is directly opposite the resultant force on K_1^+. If assumption (iii) is correct then this is the more stable arrangement; and it is seen that the net effect is an alternating ±120° rotation between layers, as required for the $2M_1$ structure (Fig. 7(*b*)). The alternative position of layer C (Fig. 7(*c*)) corresponds to the 3T structure. This does not remove K_2^+ as far as possible from K_1^+, and would not be so likely to occur as the $2M_1$ arrangement.

Other layer silicate structures—some hypotheses

The above conclusions lead to interesting speculations concerning structures related to $2M_1$ muscovite.

(*a*) *Structure of* $1M$ *muscovite*

It is easily shown that the β-angle of the separate 10 Å layers (Smith & Yoder, 1956) in $2M_1$ muscovite is 101° 28′, assuming the layers to be rotated through ±63° 36′ to the a-axis of the $2M_1$ unit cell and using the observed K^+ parameters. This will also be the β-angle of $1M$ muscovite if this has a closely similar layer structure but differs in the stacking of the layers. The *observed* value of β is 101° 35′ ± 5′, and the theoretical value is 100° 0′; so that we may conclude that the $1M$ structure is very similar to one layer of the $2M_1$ structure. Bradley (1957) has also deduced a similar monoclinic angle for $1M$ muscovite, from a hypothetical ordering, based on packing considerations, of the tetrahedral Si and Al ions. His arrangement, however, predicts that the K displacement will be at approx. 15° to the $1M$ a-axis, and requires complete ordering of Si and Al. Neither suggestion is permissible within the space group $C2/m$ suggested by Pabst (1955) for $1M$ micas since the K^+ ion is at $0, \frac{1}{2}, 0$ and the Si and Al must be completely disordered. (There can only be one, not four, general positions in the unit cell for all the tetrahedral ions). The present hypothesis sets the additional K^+ displacement along the b-axis direction, as required for $C2/m$.

The writer suggests that the unit cell for $1M$ muscovite as proposed for $1M$ micas by Pabst (1955) should be shifted by $c/2$, for convenience in comparing $1M$ and $2M_1$ micas. This places the K^+ at $0, \frac{1}{2}, \frac{1}{2}$ instead of $0, \frac{1}{2}, 0$, but these special positions are comparable in $C2/m$. For $2M_1$ muscovite ($C2/c$) the K^+ is at $0, y, \frac{1}{4}$, the counterpart of $0, \frac{1}{2}, \frac{1}{2}$ in the larger cell, whereas there is no counterpart of $0, \frac{1}{2}, 0$, which does not fix y.

If the space group proposed recently by Pabst (1955) for the $1M$ structure is correct then the tetrahedral sites must be completely disordered (i.e. four $Si_{\frac{3}{4}}Al_{\frac{1}{4}}$ sites) since there are eight tetrahedral cations and only eight general positions in the unit cell for $C2/m$. For the five other simple polymorphs (Smith & Yoder, 1956) there are twice as many general positions as there are tetrahedral cations. Hence partial ordering up to ($Si_{\frac{3}{4}}Al_{\frac{1}{4}}$ and Si) is the maximum possible, if these space groups are correct.

(*b*) *Trioctahedral layer silicates*

For the trioctahedral micas there is less misfit between the tetrahedral and octahedral layers than for dioctahedral micas, due to their larger octahedral dimensions. The brucite, $Mg(OH)_2$, lattice corresponds to a b-axis of about 9·36 Å (Brindley & MacEwan, 1953) and the tetrahedral layer to 9·30 ± 0·06 Å. The b-axis of phlogopite (and biotite) is 9·23 Å, but both

this and the octahedral layer dimensions will vary with ionic substitutions in the latter. The absence of 06*l* reflections with *l* odd confirms that there is less distortion from the ideal structures.

Lepidolite ($K.LiAl_2.Si_4O_{10}(OH)_2$) is particularly interesting because it is the only mica for which the tetrahedral positions are completely occupied by Si. This layer ($b=9{\cdot}10$ Å) should therefore fit easily to an octahedral layer containing some larger Li^+ as well as Al^{+++}; and the value of $b=9{\cdot}07$ Å (Levinson, 1953) is consistent with this. Lepidolite should therefore show little distortion of the hexagonal layer surface; and Levinson (1953) has reported the gradual disappearance of the sensitive 06*l* reflections with *l* odd as the lithium content of muscovite increases.

The analogous structure, pyrophyllite,

$$Al_2Si_4O_{10}(OH)_2\,,$$

which contains no Li^+ in the octahedral position, has a *b*-axis of 8·90 Å, and may therefore be expected to show moderate rotations of the Si–O tetrahedra. In contrast to this the talc structure, $Mg_3Si_4O_{10}(OH)_2$, with $b=9{\cdot}10$ Å appears to be one in which the Si–O tetrahedral layer ($b=9{\cdot}16$ Å) controls the structure by causing some compression of the Mg–O, OH octahedral layer ($b=9{\cdot}36$ Å approx.). The silica sheet in talc is therefore probably fully extended and undistorted.

(*c*) *Brittle micas*

In the brittle micas

(e.g. margarite, $CaAl_2.Al_2Si_2O_{10}(OH)_2$)

which are less common than normal micas, the Si:Al ratio of 1:1 in the tetrahedral layer implies a 'natural' *b*-axis for this layer of $9{\cdot}58\pm0{\cdot}06$ Å (Brindley & MacEwan, 1953). There must be considerable strain between this and the octahedral layer, and since $b=8{\cdot}92$ Å (Mauguin, 1928) even greater rotation of the tetrahedra would be expected than for muscovite.

(*d*) *Paragonite structure*

Suppose that the K^+ of muscovite could be removed and the layers collapsed without pronounced changes in the latter. An approximate calculation shows that a monovalent ion with radius less than 0·93 Å could be accommodated within the six inner oxygens. The Na^+ ion has a radius of 0·95 Å, and paragonite, $NaAl_2(Si_3Al)O_{10}(OH)_2$, is the sodium analogue of muscovite, with closely similar *a*- and *b*-axes, and giving 06*l*, *l* odd reflections. The *c*-axis of paragonite is $19{\cdot}28_5$ Å, and of muscovite is 20·09 Å, which clearly suggests that the paragonite layers have a closely similar structure to muscovite, but that the layers are in contact about the (smaller) Na^+ ion. The β-angle of paragonite is 94° 05′, approximately—not too different from muscovite for this hypothesis.

Pyrophyllite, $Al_2Si_4O_{10}(OH)_2$, with no interlayer ion also has a smaller *c*-axis (18·55 Å) than muscovite.

(*e*) *Prochlorite and corundophillite*

Steinfink (1958*a*, *b*) has discussed certain features of the prochlorite and corundophillite structures on the basis of layer dimensions, but the arguments appear to be inconsistent. It appears incorrect to state (Steinfink, 1958*b*) that 'the dimensions of the octahedral talc layer in the monoclinic polymorph are larger than in the triclinic structure, and the tetrahedral layer has to undergo a larger distortion to fit itself to its octahedral neighbour. The larger value of b_0 in prochlorite also reflects this expansion of the octahedral talc layer'. The implication is that the tetrahedral layer is distorted because it is *smaller* than the octahedral talc layer. But if we compute 'free' layer dimensions by Brindley & MacEwan's approximate formulae (1953), we find

(1) for an $Si_{\frac{3}{4}}Al_{\frac{1}{4}}$–O tetrahedral layer, $b=9{\cdot}58\pm0{\cdot}06$;
(2) for the brucite layer in prochlorite, $b=9{\cdot}06$;
(3) for the talc layer in prochlorite, $b=9{\cdot}50$.

In the *talc* layer, therefore, there should be practically no misfit between the octahedral and tetrahedral layers. It is the *brucite* layer which controls the prochlorite *b*-axis, because there is a limit to the amount which it can be stretched. The tetrahedral distortion occurs to allow the talc layer to *contract* somewhat towards the brucite layer. This is confirmed by the fact that the brucite layer is 1·85 Å thick, against 2·10 Å for brucite itself. The *c*-axis for corundophillite ($14{\cdot}36\pm0{\cdot}02$) may be significantly greater than in prochlorite ($14{\cdot}25\pm0{\cdot}02$) for this reason, and the β-angle of prochlorite may depart from the theoretical value because of the stretching of the brucite layer. It seems unlikely that ordering in these minerals can be due to the very slight dimensional difference between a network of, say, 3 Si–O and 1 Al–O tetrahedra, and of 4 $Si_{\frac{3}{4}}Al_{\frac{1}{4}}$–O tetrahedra. The explanation more probably depends on some local balance-of-charge effect (as proposed for albcites by Ferguson *et al.* (1958)) consequent upon distortion of the lattice.

A detailed structure analysis of the layer silicates should explain any departure of the observed monoclinic angle from the theoretical values, and it is therefore surprising to note some discrepancy in the data for prochlorite. Brindley, Oughton & Robinson (1950) obtained a theoretical angle of 97° 8′ 42″, and a measured angle of 97° 6′ for monoclinic chlorite. Steinfink (1958*a*), however, gives data for a monoclinic chlorite from which β(observed) = 96° 17′ ± 10′ but β(theoretical) = $\cos^{-1} -a/3/c = 97°\ 13'$.

The observed $\beta=97°\ 22'\pm6'$ and the theoretical $\beta=97°\ 8'$ for triclinic chlorite (Steinfink, 1958*b*) are in reasonable agreement, however.

Conclusion

These speculations concerning mica structures can only be tested by precise structure analyses of some or all of these minerals. For this purpose it is important

to apply adequate significance tests (Lipson & Cochran, 1953, p. 309) to bondlengths, especially if detailed interpretations are given to results obtained from few data (as, e.g. in the prochlorite analysis). The present discussion suggests that trial structures for layer silicates may now be proposed which include some degree of distortion, the amount depending on the calculated misfit of the layers, and the direction on the attractive forces due to assumed residual charges.

The mica specimen was kindly supplied by Dr A. W. Kleeman, the refractive indices determined by Dr E. R. Segnit, both of the Department of Geology, University of Adelaide. It is a pleasure to acknowledge helpful discussions with Dr K. Norrish and other colleagues during this work.

References

Berghuis, J., Haanappel, IJ. M., Potters, M., Loopstra, B. O., MacGillavry, C. H. & Veenendaal, A.L. (1955). *Acta Cryst.* **8**, 478.

Bradley, W. F. (1957). *Sixth Nat. Clay Conference Proceedings.*

Bragg, W. L. (1937). *Atomic Structure of Minerals.* London: Oxford University Press.

Bragg, W. L. & West, J. (1929). *Z. Kristallogr.* **69**, 118.

Brindley, G. W. (1951). *X-ray Identification of Clay Minerals*, p. 35. London: The Mineralogical Soc.

Brindley, G.W. & MacEwan, D.M.C. (1953). Ceramics; a symposium, *Brit. Cer. Soc.* p. 15.

Brindley, G. W., Oughton, B. M. & Robinson, K. (1950). *Acta Cryst.* **3**, 408.

Cruickshank, D. W. J. (1949). *Acta Cryst.* **2**, 65.

Ferguson, R. B., Traill, R. J. & Taylor, W. H. (1958). *Acta Cryst.* **11**, 331.

Gatineau, L. & Méring, J. (1958). *Clay Min. Bull.* **3**, 238.

Harrison, F. W. & Brindley, G. W. (1957). *Acta Cryst.* **10**, 77.

Hendricks, S. B. & Jefferson, M. E. (1939). *Amer. Min.* **24**, 729.

Jackson, W. W. & West, J. (1930). *Z. Kristallogr.* **76**, 211.

Jackson, W. W. & West, J. (1933). *Z. Kristallogr.* **85**, 160.

Levinson, A. A. (1953). *Amer. Min.* **38**, 88.

Lipson, H. & Cochran, W. (1953). *The Determination of Crystal Structures.* London: Bell.

Mathieson, A. McL. (1958). *Amer. Min.* **43**, 216.

Mathieson, A. McL. & Walker, G. F. (1954). *Amer. Min.* **94**, 231.

Mauguin, C. (1928). *C. R. Acad. Sci. Paris*, **185**, 288.

Newnham, R. E. & Brindley, G. W. (1956). *Acta Cryst.* **9**, 759.

Pabst, A. (1955). *Amer. Min.* **40**, 967.

Pauling, L. (1930). *Proc. Nat. Acad. Sci. Wash.* **16**, 123.

Radoslovich, E. W. (1959). *Nature, Lond.* **183**, 253.

Smith, J. V. (1954). *Acta Cryst.* **7**, 479.

Smith, J. V. & Yoder, H. S. (1956). *Min. Mag.* **XXXI**, 209.

Steinfink, H. (1958*a*). *Acta Cryst.* **11**, 191.

Steinfink, H. (1958*b*). *Acta Cryst.* **11**, 195.

Steinfink, H. & Brunton, G. (1956). *Acta Cryst.* **9**, 487.

Verhoogen, J. (1958). *Amer. Min.* **43**, 552.

Viervoll, H. & Ørgrim, O. (1949). *Acta Cryst.* **2**, 277.

Whittaker, E. J. W. (1949). *Acta Cryst.* **2**, 312.

Whittaker, E. J. W. (1956). *Acta Cryst.* **9**, 855.

Yoder, H. S. & Eugster, H. P. (1955). *Geochim. Cosmochim. Acta* **8**, 225.

Acta Cryst. (1960). **13**, 932

Morphology of Synthetic Submicroscopic Crystals of α and γFeOOH and of γFe_2O_3 Prepared from FeOOH

By G. W. van Oosterhout

Philips Research Laboratories, N. V. Philips' Gloeilampenfabrieken, Eindhoven, The Netherlands

(*Received* 30 *November* 1959)

The orientation of the needle axis of synthetic acicular crystals of α and γFeOOH with respect to the unit cell has been determined by selected-area electron diffraction. The needle axis is [001] for αFeOOH ($c = 3{\cdot}03$ Å) and γFeOOH ($c = 3{\cdot}06$ Å) and [110] for γFe_2O_3 prepared either by dehydration of γFeOOH or by reduction of αFeOOH or γFeOOH followed by oxidation.

The results are compared with previous work on this subject and the possible causes of the discrepancies between the results of Osmond and of Campbell and those obtained in the present paper are discussed.

Introduction

Knowledge of the orientation of the needle axis of acicular γFe_2O_3 with respect to the unit cell is necessary for a discussion of the magnetic properties of these crystals as they are used in magnetic recording devices. Several papers have already been published on this subject (Osmond, 1953; Campbell, 1957*a*, *b*, *c*). Because they report contradictory results it was considered desirable to publish our own results with a discussion of those of the other authors in order to trace the origin of these discrepancies.